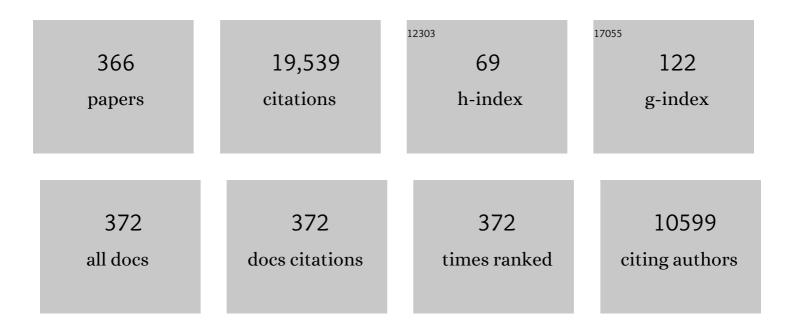
David C Dunand

List of Publications by Year in descending order

Source: https://exaly.com/author-pdf/227865/publications.pdf Version: 2024-02-01



#	Article	IF	CITATIONS
1	Porous Metals and Metallic Foams: Current Status and Recent Developments. Advanced Engineering Materials, 2008, 10, 775-787.	1.6	676
2	Precipitation strengthening at ambient and elevated temperatures of heat-treatable Al(Sc) alloys. Acta Materialia, 2002, 50, 4021-4035.	3.8	645
3	Porous NiTi for bone implants: A review. Acta Biomaterialia, 2008, 4, 773-782.	4.1	483
4	Criteria for developing castable, creep-resistant aluminum-based alloys – A review. International Journal of Materials Research, 2006, 97, 246-265.	0.8	431
5	Precipitation evolution in Al–0.1Sc, Al–0.1Zr and Al–0.1Sc–0.1Zr (at.%) alloys during isochronal aging. Acta Materialia, 2010, 58, 5184-5195.	3.8	408
6	Mechanical properties of Al(Sc,Zr) alloys at ambient and elevated temperatures. Acta Materialia, 2003, 51, 4803-4814.	3.8	385
7	Giant magnetic-field-induced strains in polycrystalline Ni–Mn–Ga foams. Nature Materials, 2009, 8, 863-866.	13.3	332
8	Coarsening resistance at 400 °C of precipitation-strengthened Al–Zr–Sc–Er alloys. Acta Materialia, 2011, 59, 7029-7042.	3.8	315
9	Microstructure and mechanical properties of Al-Mg-Zr alloys processed by selective laser melting. Acta Materialia, 2018, 153, 35-44.	3.8	315
10	Size Effects on Magnetic Actuation in Niâ€Mnâ€Ga Shapeâ€Memory Alloys. Advanced Materials, 2011, 23, 216-232.	11.1	312
11	Processing of Titanium Foams. Advanced Engineering Materials, 2004, 6, 369-376.	1.6	294
12	Ambient- and high-temperature mechanical properties of isochronally aged Al–0.06Sc, Al–0.06Zr and Al–0.06Sc–0.06Zr (at.%) alloys. Acta Materialia, 2011, 59, 943-954.	3.8	269
13	Freeze casting – A review of processing, microstructure and properties via the open data repository, FreezeCasting.net. Progress in Materials Science, 2018, 94, 243-305.	16.0	269
14	Precipitation evolution in Al–Zr and Al–Zr–Ti alloys during aging at 450–600°C. Acta Materialia, 2008, 56, 1182-1195.	3.8	246
15	Precipitation evolution in Al–Zr and Al–Zr–Ti alloys during isothermal aging at 375–425°C. Acta Materialia, 2008, 56, 114-127.	3.8	239
16	Directionally freeze-cast titanium foam with aligned, elongated pores. Acta Materialia, 2008, 56, 105-113.	3.8	220
17	SMARTS - a spectrometer for strain measurement in engineering materials. Applied Physics A: Materials Science and Processing, 2002, 74, s1707-s1709.	1.1	219
18	Hybrid bone implants: Self-assembly of peptide amphiphile nanofibers within porous titanium. Biomaterials, 2008, 29, 161-171.	5.7	216

#	Article	IF	CITATIONS
19	Plasticity and damage in aluminum syntactic foams deformed under dynamic and quasi-static conditions. Materials Science & Engineering A: Structural Materials: Properties, Microstructure and Processing, 2005, 391, 408-417.	2.6	208
20	High strength, low stiffness, porous NiTi with superelastic properties. Acta Biomaterialia, 2005, 1, 705-716.	4.1	206
21	Improving aging and creep resistance in a dilute Al–Sc alloy by microalloying with Si, Zr and Er. Acta Materialia, 2014, 63, 73-85.	3.8	203
22	A bioactive titanium foam scaffold for bone repair. Acta Biomaterialia, 2005, 1, 523-533.	4.1	175
23	Phase transformation and thermal expansion of Cu/ZrW ₂ O ₈ metal matrix composites. Journal of Materials Research, 1999, 14, 780-789.	1.2	172
24	Metallic Architectures from 3Dâ€Printed Powderâ€Based Liquid Inks. Advanced Functional Materials, 2015, 25, 6985-6995.	7.8	164
25	Structural evolution of nanoporous gold during thermal coarsening. Acta Materialia, 2012, 60, 4972-4981.	3.8	163
26	Role of silicon in accelerating the nucleation of Al3(Sc,Zr) precipitates in dilute Al–Sc–Zr alloys. Acta Materialia, 2012, 60, 4740-4752.	3.8	161
27	Shape-memory NiTi foams produced by replication of NaCl space-holders. Acta Biomaterialia, 2008, 4, 1996-2007.	4.1	159
28	Nucleation and Precipitation Strengthening in Dilute Al-Ti and Al-Zr Alloys. Metallurgical and Materials Transactions A: Physical Metallurgy and Materials Science, 2007, 38, 2552-2563.	1.1	156
29	Effect of laser rescanning on the grain microstructure of a selective laser melted Al-Mg-Zr alloy. Materials Characterization, 2018, 143, 34-42.	1.9	156
30	Effect of Mg addition on the creep and yield behavior of an Al–Sc alloy. Acta Materialia, 2003, 51, 4751-4760.	3.8	155
31	Printed Origami Structures. Advanced Materials, 2010, 22, 2251-2254.	11.1	144
32	Effect of Er additions on ambient and high-temperature strength of precipitation-strengthened Al–Zr–Sc–Si alloys. Acta Materialia, 2012, 60, 3643-3654.	3.8	138
33	Load partitioning in aluminum syntactic foams containing ceramic microspheres. Acta Materialia, 2006, 54, 1501-1511.	3.8	133
34	Creep properties and microstructure of a precipitation-strengthened ferritic Fe–Al–Ni–Cr alloy. Acta Materialia, 2014, 71, 89-99.	3.8	133
35	Effects of substituting rare-earth elements for scandium in a precipitation-strengthened Al–0.08at. %Sc alloy. Scripta Materialia, 2006, 55, 437-440.	2.6	129
36	Mechanical properties of a density-graded replicated aluminum foam. Materials Science & Engineering A: Structural Materials: Properties, Microstructure and Processing, 2008, 489, 439-443.	2.6	128

#	Article	IF	CITATIONS
37	Ductile Bulk Metallic Glass Foams. Advanced Materials, 2005, 17, 484-486.	11.1	123
38	Load partitioning between ferrite and cementite during elasto-plastic deformation of an ultrahigh-carbon steel. Acta Materialia, 2007, 55, 1999-2011.	3.8	123
39	Effects of Ti additions on the nanostructure and creep properties of precipitation-strengthened Al–Sc alloys. Acta Materialia, 2005, 53, 4225-4235.	3.8	122
40	Shape-memory NiTi foams produced by solid-state replication with NaF. Intermetallics, 2007, 15, 1612-1622.	1.8	116
41	Microstructure and mechanical properties of a precipitation-strengthened Al-Zr-Sc-Er-Si alloy with a very small Sc content. Acta Materialia, 2018, 144, 80-91.	3.8	115
42	Model for creep threshold stress in precipitation-strengthened alloys with coherent particles. Scripta Materialia, 2002, 47, 503-508.	2.6	114
43	Erbium and ytterbium solubilities and diffusivities in aluminum as determined by nanoscale characterization of precipitates. Acta Materialia, 2009, 57, 4081-4089.	3.8	114
44	Mechanical properties of directionally freeze-cast titanium foams. Acta Materialia, 2011, 59, 146-158.	3.8	114
45	Microstructure and mechanical properties of a 5754 aluminum alloy modified by Sc and Zr additions. Materials Science & Engineering A: Structural Materials: Properties, Microstructure and Processing, 2002, 338, 8-16.	2.6	113
46	Evolution of nanoscale precipitates in Al microalloyed with Sc and Er. Acta Materialia, 2009, 57, 4022-4031.	3.8	111
47	Numerical modeling of pore size and distribution in foamed titanium. Mechanics of Materials, 2006, 38, 933-944.	1.7	107
48	Strain and texture evolution during mechanical loading of a crack tip in martensitic shape-memory NiTi. Acta Materialia, 2007, 55, 3929-3942.	3.8	105
49	Effects of Yb and Zr microalloying additions on the microstructure and mechanical properties of dilute Al–Sc alloys. Acta Materialia, 2011, 59, 7615-7626.	3.8	105
50	Criteria for developing castable, creep-resistant aluminum-based alloys – A review. International Journal of Materials Research, 2022, 97, 246-265.	0.1	105
51	Processing and structure of open-celled amorphous metal foams. Scripta Materialia, 2005, 52, 335-339.	2.6	104
52	3D ink-extrusion additive manufacturing of CoCrFeNi high-entropy alloy micro-lattices. Nature Communications, 2019, 10, 904.	5.8	104
53	Multicomponent γ'-strengthened Co-based superalloys with increased solvus temperatures and reduced mass densities. Acta Materialia, 2018, 147, 284-295.	3.8	100
54	Synthesis, structure, and mechanical properties of Ni–Al and Ni–Cr–Al superalloy foams. Acta Materialia, 2004, 52, 1283-1295.	3.8	96

#	Article	IF	CITATIONS
55	Titanium foams produced by solid-state replication of NaCl powders. Materials Science & Engineering A: Structural Materials: Properties, Microstructure and Processing, 2010, 528, 691-697.	2.6	93
56	Synchrotron X-ray study of bulk lattice strains in externally loaded Cu-Mo composites. Metallurgical and Materials Transactions A: Physical Metallurgy and Materials Science, 2000, 31, 2949-2962.	1.1	90
57	Increasing Magnetoplasticity in Polycrystalline Ni-Mn-Ga by Reducing Internal Constraints through Porosity. Physical Review Letters, 2007, 99, 247201.	2.9	88
58	Phase fraction, texture and strain evolution in superelastic NiTi and NiTi–TiC composites investigated by neutron diffraction. Acta Materialia, 1999, 47, 3353-3366.	3.8	87
59	Syntactic bulk metallic glass foam. Applied Physics Letters, 2004, 84, 1108-1110.	1.5	86
60	Towards an integrated materials characterization toolbox. Journal of Materials Research, 2011, 26, 1341-1383.	1.2	84
61	Morphological and topological analysis of coarsened nanoporous gold by x-ray nanotomography. Applied Physics Letters, 2010, 96, 043122.	1.5	82
62	Modeling the creep threshold stress due to climb of a dislocation in the stress field of a misfitting precipitate. Acta Materialia, 2011, 59, 5125-5134.	3.8	81
63	Strengthening mechanisms in aluminum containing coherent Al3Sc precipitates and incoherent Al2O3 dispersoids. Acta Materialia, 2007, 55, 1299-1308.	3.8	80
64	Ferritic Alloys with Extreme Creep Resistance via Coherent Hierarchical Precipitates. Scientific Reports, 2015, 5, 16327.	1.6	80
65	Effects of Pore Morphology and Bone Ingrowth on Mechanical Properties of Microporous Titanium as an Orthopaedic Implant Material. Materials Transactions, 2004, 45, 1124-1131.	0.4	79
66	Plasticity and damage in cellular amorphous metals. Acta Materialia, 2005, 53, 4427-4440.	3.8	77
67	Effect of reinforcement connectivity on the elasto-plastic behavior of aluminum composites containing sub-micron alumina particles. Acta Materialia, 2003, 51, 6105-6121.	3.8	75
68	Creep properties of coarse-grained Al(Sc) alloys at 300°C. Scripta Materialia, 1999, 40, 691-696.	2.6	74
69	Synthesis of nickel–aluminide foams by pack-aluminization of nickel foams. Intermetallics, 2001, 9, 581-589.	1.8	74
70	Titanium with controllable pore fractions by thermoreversible gelcasting of TiH2. Acta Materialia, 2008, 56, 5147-5157.	3.8	72
71	Mechanical properties and optimization of the aging of a dilute Al-Sc-Er-Zr-Si alloy with a high Zr/Sc ratio. Acta Materialia, 2016, 119, 35-42.	3.8	71
72	Creep of magnesium strengthened with high volume fractions of yttria dispersoids. Materials Science & Engineering A: Structural Materials: Properties, Microstructure and Processing, 2001, 300, 235-244.	2.6	69

#	Article	IF	CITATIONS
73	Iron and Nickel Cellular Structures by Sintering of 3Dâ€Printed Oxide or Metallic Particle Inks. Advanced Engineering Materials, 2017, 19, 1600365.	1.6	68
74	Shape memory and superelasticity in polycrystalline Cu–Al–Ni microwires. Applied Physics Letters, 2009, 95, .	1.5	67
75	Density-Graded Cellular Aluminum. Advanced Engineering Materials, 2006, 8, 805-809.	1.6	66
76	Creep resistance of cast and aged Al–0.1Zr and Al–0.1Zr–0.1Ti (at.%) alloys at 300–400°C. Scripta Materialia, 2008, 59, 387-390.	2.6	66
77	Iron Oxide Photoelectrode with Multidimensional Architecture for Highly Efficient Photoelectrochemical Water Splitting. Angewandte Chemie - International Edition, 2017, 56, 6583-6588.	7.2	66
78	Ni-Mn-Ga micro-trusses via sintering of 3D-printed inks containing elemental powders. Acta Materialia, 2018, 143, 20-29.	3.8	66
79	Core–shell nanoscale precipitates in Al–0.06 at.% Sc microalloyed with Tb, Ho, Tm or Lu. Acta Materialia, 2010, 58, 134-145.	3.8	64
80	A new model to simulate the elastic properties of mineralized collagen fibril. Biomechanics and Modeling in Mechanobiology, 2011, 10, 147-160.	1.4	64
81	Sintering of micro-trusses created by extrusion-3D-printing of lunar regolith inks. Acta Astronautica, 2018, 143, 1-8.	1.7	64
82	Fatigue crack-growth in shape-memory NiTi and NiTi–TiC composites. Materials Science & Engineering A: Structural Materials: Properties, Microstructure and Processing, 2000, 289, 208-216.	2.6	63
83	Creep properties of Al3Sc and Al3(Sc, X) intermetallics. Acta Materialia, 2000, 48, 3477-3487.	3.8	63
84	Microstructure evolution during solid-state foaming of titanium. Composites Science and Technology, 2003, 63, 2311-2316.	3.8	63
85	Microstructural evolution and creep properties of precipitation-strengthened Al–0.06Sc–0.02Gd and Al–0.06Sc–0.02Yb (at.%) alloys. Acta Materialia, 2011, 59, 5224-5237.	3.8	63
86	Role of silicon in the precipitation kinetics of dilute Al-Sc-Er-Zr alloys. Materials Science & Engineering A: Structural Materials: Properties, Microstructure and Processing, 2016, 677, 485-495.	2.6	63
87	Whisker alignment of Ti–6Al–4V/TiB composites during deformation by transformation superplasticity. International Journal of Plasticity, 2001, 17, 317-340.	4.1	61
88	Atom-probe tomographic study of γ/γ′ interfaces and compositions in an aged Co–Al–W superalloy. Scripta Materialia, 2013, 68, 563-566.	2.6	61
89	Effect of vanadium micro-alloying on the microstructural evolution and creep behavior of Al-Er-Sc-Zr-Si alloys. Acta Materialia, 2017, 124, 501-512.	3.8	61
90	Cast near-eutectic Al-12.5†wt.% Ce alloy with high coarsening and creep resistance. Materials Science & Engineering A: Structural Materials: Properties, Microstructure and Processing, 2019, 767, 138440.	2.6	61

#	Article	IF	CITATIONS
91	Thermal mismatch dislocations produced by large particles in a strain-hardening matrix. Materials Science & Engineering A: Structural Materials: Properties, Microstructure and Processing, 1991, 135, 179-184.	2.6	60
92	Effects of titanium substitutions for aluminum and tungsten in Co-10Ni-9Al-9W (at%) superalloys. Materials Science & Engineering A: Structural Materials: Properties, Microstructure and Processing, 2017, 705, 122-132.	2.6	60
93	Transformation-mismatch superplasticity in reinforced and unreinforced titanium. Acta Materialia, 1996, 44, 1063-1076.	3.8	59
94	Reactive Synthesis of Aluminide Intermetallics. Materials and Manufacturing Processes, 1995, 10, 373-403.	2.7	58
95	Effects of Mo and Mn microadditions on strengthening and over-aging resistance of nanoprecipitation-strengthened Al-Zr-Sc-Er-Si alloys. Acta Materialia, 2019, 165, 1-14.	3.8	58
96	Sustainability through alloy design: Challenges and opportunities. Progress in Materials Science, 2021, 117, 100722.	16.0	58
97	Effect of thermal history on the superplastic expansion of argon-filled pores in titanium: Part I kinetics and microstructure. Acta Materialia, 2004, 52, 2269-2278.	3.8	57
98	Atom probe tomographic study of a friction-stir-processed Al–Mg–Sc alloy. Acta Materialia, 2012, 60, 7078-7089.	3.8	57
99	Creep- and coarsening properties of Al–0.06at.% Sc–0.06at.% Ti at 300–450°C. Acta Materialia, 2008, 56 4369-4377.	' 3.8	56
100	γ+γ′ microstructures in the Co-Ta-V and Co-Nb-V ternary systems. Acta Materialia, 2018, 151, 137-148.	3.8	56
101	Nanoscale precipitation and mechanical properties of Al-0.06 at.% Sc alloys microalloyed with Yb or Gd. Journal of Materials Science, 2006, 41, 7814-7823.	1.7	55
102	Roles of impurities on precipitation kinetics of dilute Al–Sc alloys. Materials Science & Engineering A: Structural Materials: Properties, Microstructure and Processing, 2010, 527, 3501-3509.	2.6	55
103	Influence of ruthenium on microstructural evolution in a model Co Al W superalloy. Acta Materialia, 2016, 117, 135-145.	3.8	54
104	Comparison between dislocation dynamics model predictions and experiments in precipitation-strengthened Al–Li–Sc alloys. Acta Materialia, 2014, 79, 382-395.	3.8	53
105	Finite-element analysis of thermal expansion and thermal mismatch stresses in a Cu–60vol%ZrW2O8 composite. Composites Science and Technology, 2004, 64, 1895-1898.	3.8	52
106	Microstructural and creep properties of boron- and zirconium-containing cobalt-based superalloys. Materials Science & Engineering A: Structural Materials: Properties, Microstructure and Processing, 2017, 682, 260-269.	2.6	52
107	Chemistry and structure of core/double-shell nanoscale precipitates in Al–6.5Li–0.07Sc–0.02Yb (at.%). Acta Materialia, 2011, 59, 3398-3409.	3.8	51
108	Effect of Ag–Au composition and acid concentration on dealloying front velocity and cracking during nanoporous gold formation. Acta Materialia, 2013, 61, 5561-5570.	3.8	51

#	Article	IF	CITATIONS
109	Iron Oxide Photoelectrode with Multidimensional Architecture for Highly Efficient Photoelectrochemical Water Splitting. Angewandte Chemie, 2017, 129, 6683-6688.	1.6	51
110	Increasing the creep resistance of Fe-Ni-Al-Cr superalloys via Ti additions by optimizing the B2/L21 ratio in composite nano-precipitates. Acta Materialia, 2018, 157, 142-154.	3.8	51
111	Measurement and modeling of creep in open-cell NiAl foams. Metallurgical and Materials Transactions A: Physical Metallurgy and Materials Science, 2003, 34, 2353-2363.	1.1	50
112	Creep of Al-Sc Microalloys with Rare-Earth Element Additions. Materials Science Forum, 2006, 519-521, 1035-1040.	0.3	49
113	Effect of Al, Ti and Cr additions on the γ-γ' microstructure of W-free Co-Ta-V-Based superalloys. Acta Materialia, 2019, 172, 44-54.	3.8	49
114	Microstructure of Fe2O3 scaffolds created by freeze-casting and sintering. Materials Letters, 2015, 142, 56-59.	1.3	48
115	3D macroporous electrode and high-performance in lithium-ion batteries using SnO2 coated on Cu foam. Scientific Reports, 2016, 6, 18626.	1.6	48
116	Copper-zirconium tungstate composites exhibiting low and negative thermal expansion influenced by reinforcement phase transformations. Metallurgical and Materials Transactions A: Physical Metallurgy and Materials Science, 2004, 35, 1159-1165.	1.1	47
117	Load partitioning during compressive loading of a Mg/MgB2 composite. Acta Materialia, 2007, 55, 3467-3478.	3.8	47
118	Titanium foam-bioactive nanofiber hybrids for bone regeneration. Journal of Tissue Engineering and Regenerative Medicine, 2008, 2, 455-462.	1.3	47
119	Non-isothermal transformation-mismatch plasticity: modeling and experiments on Ti–6Al–4V. Acta Materialia, 2001, 49, 199-210.	3.8	46
120	Porous and Foamed Amorphous Metals. MRS Bulletin, 2007, 32, 639-643.	1.7	46
121	Shape-memory NiTi with two-dimensional networks of micro-channels. Acta Biomaterialia, 2011, 7, 1862-1872.	4.1	46
122	Effect of titanium additions upon microstructure and properties of precipitation-strengthened Fe-Ni-Al-Cr ferritic alloys. Acta Materialia, 2017, 128, 103-112.	3.8	46
123	Porous Titanium by Electroâ€chemical Dissolution of Steel Spaceâ€holders. Advanced Engineering Materials, 2008, 10, 820-825.	1.6	45
124	Lattice strain evolution and load partitioning during creep of a Ni-based superalloy single crystal with rafted γ′ microstructure. Acta Materialia, 2017, 135, 77-87.	3.8	45
125	Titanium with aligned, elongated pores for orthopedic tissue engineering applications. Journal of Biomedical Materials Research - Part A, 2008, 84A, 402-412.	2.1	44
126	Creep properties and precipitate evolution in Al–Li alloys microalloyed with Sc and Yb. Materials Science & Engineering A: Structural Materials: Properties, Microstructure and Processing, 2012, 550, 300-311.	2.6	44

#	Article	IF	CITATIONS
127	In situ imaging of dealloying during nanoporous gold formation by transmission X-ray microscopy. Acta Materialia, 2013, 61, 1118-1125.	3.8	44
128	Superelasticity by reversible variants reorientation in a Ni–Mn–Ga microwire with bamboo grains. Acta Materialia, 2015, 99, 373-381.	3.8	44
129	Lattice parameter misfit evolution during creep of a cobalt-based superalloy single crystal with cuboidal and rafted gamma-prime microstructures. Acta Materialia, 2017, 136, 118-125.	3.8	44
130	Elastic phase-strain distribution in a particulate-reinforced metal-matrix composite deforming by slip or creep. Metallurgical and Materials Transactions A: Physical Metallurgy and Materials Science, 1999, 30, 2989-2997.	1.1	42
131	Effect of pore architecture on magnetic-field-induced strain in polycrystalline Ni–Mn–Ga. Acta Materialia, 2011, 59, 2229-2239.	3.8	42
132	Dislocation-based modeling of long-term creep behaviors of Grade 91 steels. Acta Materialia, 2018, 149, 19-28.	3.8	42
133	Transformation superplasticity of zirconium. Metallurgical and Materials Transactions A: Physical Metallurgy and Materials Science, 1998, 29, 2571-2582.	1.1	41
134	Mechanical Properties of Cast Ti-6Al-4V Lattice Block Structures. Metallurgical and Materials Transactions A: Physical Metallurgy and Materials Science, 2008, 39, 441-449.	1.1	41
135	Preparation and Characterization of Directionally Freeze-cast Copper Foams. Metals, 2012, 2, 265-273.	1.0	40
136	Permeability measurements and modeling of topology-optimized metallic 3-D woven lattices. Acta Materialia, 2014, 81, 326-336.	3.8	40
137	Effect of directional solidification on texture and magnetic-field-induced strain in Ni–Mn–Ga foams with coarse grains. Acta Materialia, 2015, 86, 95-101.	3.8	40
138	Microstructural evolution and high-temperature strength of a γ(f.c.c.)/γ'(L12) Co–Al–W–Ti–B superalloy. Acta Materialia, 2019, 174, 427-438.	3.8	40
139	Microstructure and mechanical properties of Ti/W and Ti–6Al–4V/W composites fabricated by powder-metallurgy. Materials Science & Engineering A: Structural Materials: Properties, Microstructure and Processing, 2003, 344, 103-112.	2.6	39
140	3D morphological evolution of porous titanium by x-ray micro- and nano-tomography. Journal of Materials Research, 2013, 28, 2444-2452.	1.2	39
141	Mechanical and magnetic behavior of oligocrystalline Ni–Mn–Ga microwires. Journal of Alloys and Compounds, 2015, 624, 226-233.	2.8	39
142	Ambient- and elevated-temperature strengthening by Al3Zr-Nanoprecipitates and Al3Ni-Microfibers in a cast Al-2.9Ni-0.11Zr-0.02Si-0.005Er (at.%) alloy. Materials Science & Engineering A: Structural Materials: Properties, Microstructure and Processing, 2019, 759, 78-89.	2.6	39
143	Niâ€Moâ€Cr Foams Processed by Casting Replication of Sodium Aluminate Preforms. Advanced Engineering Materials, 2008, 10, 379-383.	1.6	38
144	Cavitation-resistant intergranular precipitates enhance creep performance of Î,′-strengthened Al-Cu based alloys. Acta Materialia, 2022, 228, 117788.	3.8	38

#	Article	IF	CITATIONS
145	Composition profiles within Al3Li and Al3Scâ^•Al3Li nanoscale precipitates in aluminum. Applied Physics Letters, 2008, 92, .	1.5	37
146	Bulk gold with hierarchical macro-, micro- and nano-porosity. Materials Science & Engineering A: Structural Materials: Properties, Microstructure and Processing, 2011, 528, 2401-2406.	2.6	37
147	Effect of tungsten additions on the mechanical properties of Ti-6Al-4V. Materials Science & Engineering A: Structural Materials: Properties, Microstructure and Processing, 2005, 396, 99-106.	2.6	36
148	Microstructure and compressive behavior of ice-templated copper foams with directional, lamellar pores. Materials Science & Engineering A: Structural Materials: Properties, Microstructure and Processing, 2017, 679, 435-445.	2.6	36
149	NiTi-Nb micro-trusses fabricated via extrusion-based 3D-printing of powders and transient-liquid-phase sintering. Acta Biomaterialia, 2018, 76, 359-370.	4.1	36
150	Effects of Zn and Cr additions on precipitation and creep behavior of a dilute Al–Zr–Er–Si alloy. Acta Materialia, 2019, 181, 249-261.	3.8	35
151	Effects of Cr on the properties of multicomponent cobalt-based superalloys with ultra high <mml:math <br="" xmlns:mml="http://www.w3.org/1998/Math/MathML">altimg="si1.svg"><mml:mi>(mml:mi>î³</mml:mi><mml:mo>'</mml:mo></mml:math> volume fraction. lournal of Allovs and Compounds. 2020. 832. 154790.	2.8	35
152	Effect of tungsten dissolution on the mechanical properties of Ti–W composites. Journal of Alloys and Compounds, 2005, 390, 62-66.	2.8	34
153	Shape-memory NiTi–Nb foams. Journal of Materials Research, 2009, 24, 2107-2117.	1.2	34
154	Microstructure and Mechanical Properties of Reticulated Titanium Scrolls. Advanced Engineering Materials, 2011, 13, 1122-1127.	1.6	34
155	3D interconnected SnO ₂ -coated Cu foam as a high-performance anode for lithium-ion batteryÂapplications. RSC Advances, 2014, 4, 58059-58063.	1.7	34
156	Aging- and creep-resistance of a cast hypoeutectic Al-6.9Ce-9.3Mg (wt.%) alloy. Materials Science & Engineering A: Structural Materials: Properties, Microstructure and Processing, 2020, 786, 139398.	2.6	34
157	Mn and Mo additions to a dilute Al-Zr-Sc-Er-Si-based alloy to improve creep resistance through solid-solution- and precipitation-strengthening. Acta Materialia, 2020, 194, 60-67.	3.8	34
158	Solid-state foaming of titanium by hydrogen-induced internal-stress superplasticity. Scripta Materialia, 2003, 49, 879-883.	2.6	33
159	Finite element modeling of creep deformation in cellular metals. Acta Materialia, 2007, 55, 3825-3834.	3.8	33
160	Synthesis, structure and mechanical properties of ice-templated tungsten foams. Journal of Materials Research, 2016, 31, 753-764.	1.2	33
161	Effect of tungsten concentration on microstructures of Co-10Ni-6Al-(0,2,4,6)W-6Ti (at%) cobalt-based superalloys. Materials Science & Engineering A: Structural Materials: Properties, Microstructure and Processing, 2017, 700, 481-486.	2.6	33
162	Microstructure and Processing of 3D Printed Tungsten Microlattices and Infiltrated W–Cu Composites. Advanced Engineering Materials, 2018, 20, 1800354.	1.6	33

#	Article	IF	CITATIONS
163	Structural evolution of directionally freeze-cast iron foams during oxidation/reduction cycles. Acta Materialia, 2019, 162, 90-102.	3.8	33
164	Microstructure and defects in a Ni-Cr-Al-Ti γ/γ' model superalloy processed by laser powder bed fusion. Materials and Design, 2021, 201, 109531.	3.3	32
165	Structure and mechanical properties of Ti–6Al–4V with a replicated network of elongated pores. Acta Materialia, 2011, 59, 640-650.	3.8	31
166	Mechanical anisotropy of shape-memory NiTi with two-dimensional networks of micro-channels. Acta Materialia, 2011, 59, 4616-4630.	3.8	30
167	In Operando Strain Measurement of Bicontinuous Siliconâ€Coated Nickel Inverse Opal Anodes for Liâ€lon Batteries. Advanced Energy Materials, 2015, 5, 1500466.	10.2	30
168	Effect of directional solidification and porosity upon the superelasticity of Cu–Al–Ni shape-memory alloys. Materials & Design, 2015, 80, 28-35.	5.1	30
169	γ'-(L12) precipitate evolution during isothermal aging of a Co Al W Ni superalloy. Acta Materialia, 2019, 164, 654-662.	3.8	30
170	Elasto-plastic load transfer in bulk metallic glass composites containing ductile particles. Metallurgical and Materials Transactions A: Physical Metallurgy and Materials Science, 2003, 34, 1787-1797.	1.1	29
171	Effect of thermal history on the superplastic expansion of argon-filled pores in titanium: Part II modeling of kinetics. Acta Materialia, 2004, 52, 2279-2291.	3.8	29
172	Power-law creep in near-equiatomic nickel–titanium alloys. Scripta Materialia, 2007, 57, 377-380.	2.6	29
173	Iron foams created by directional freeze casting of iron oxide, reduction and sintering. Materials Letters, 2017, 191, 112-115.	1.3	29
174	Transformation superplasticity of iron and Fe/TiC metal matrix composites. Metallurgical and Materials Transactions A: Physical Metallurgy and Materials Science, 1998, 29, 565-575.	1.1	28
175	Porous NiTi by creep expansion of argon-filled pores. Materials Science & Engineering A: Structural Materials: Properties, Microstructure and Processing, 2009, 523, 70-76.	2.6	28
176	Rafting and elastoplastic deformation of superalloys studied by neutronÂdiffraction. Scripta Materialia, 2017, 134, 110-114.	2.6	28
177	Atom Probe Tomographic Studies of Precipitation in Al-0.1Zr-0.1Ti (at.%) Alloys. Microscopy and Microanalysis, 2007, 13, 503-516.	0.2	27
178	Effects of Sb micro-alloying on precipitate evolution and mechanical properties of a dilute Al-Sc-Zr alloy. Materials Science & Engineering A: Structural Materials: Properties, Microstructure and Processing, 2017, 680, 64-74.	2.6	27
179	Pressure-Induced Transformation Plasticity of H2Olce. Physical Review Letters, 2001, 86, 668-671.	2.9	26
180	Morphological analysis of pores in directionally freeze-cast titanium foams. Journal of Materials Research, 2009, 24, 117-124.	1.2	26

#	Article	IF	CITATIONS
181	Effects of strut geometry and pore fraction on creep properties of cellular materials. Acta Materialia, 2009, 57, 1373-1384.	3.8	26
182	Ti–6Al–4V with micro- and macropores produced by powder sintering and electrochemical dissolution of steel wires. Materials Science & Engineering A: Structural Materials: Properties, Microstructure and Processing, 2010, 527, 849-853.	2.6	26
183	Processing of NiTi Foams by Transient Liquid Phase Sintering. Journal of Materials Engineering and Performance, 2011, 20, 511-516.	1.2	26
184	Microstructure and mechanical properties of as-cast quasibinary NiTi–Nb eutectic alloy. Materials Science & Engineering A: Structural Materials: Properties, Microstructure and Processing, 2015, 627, 360-368.	2.6	26
185	Precipitate Evolution and Creep Behavior of a W-Free Co-based Superalloy. Metallurgical and Materials Transactions A: Physical Metallurgy and Materials Science, 2016, 47, 6090-6096.	1.1	26
186	Atom probe tomography study of Fe-Ni-Al-Cr-Ti ferritic steels with hierarchically-structured precipitates. Acta Materialia, 2018, 144, 707-715.	3.8	26
187	Effects of Si and Fe micro-additions on the aging response of a dilute Al-0.08Zr-0.08Hf-0.045Erâ€⁻at.% alloy. Materials Characterization, 2019, 147, 72-83.	1.9	26
188	Microstructure and porosity evolution during sintering of Ni-Mn-Ga wires printed from inks containing elemental powders. Intermetallics, 2019, 104, 113-123.	1.8	26
189	Evolution of dealloying induced strain in nanoporous gold crystals. Nanoscale, 2017, 9, 5686-5693.	2.8	25
190	Effects of Nb and Ta additions on the strength and coarsening resistance of precipitation-strengthened Al-Zr-Sc-Er-Si alloys. Materials Characterization, 2018, 141, 260-266.	1.9	25
191	Enhanced densification of Ti–6Al–4V powders by transformation-mismatch plasticity. Acta Materialia, 2010, 58, 3851-3859.	3.8	24
192	Magnetic-field-induced recovery strain in polycrystalline Ni–Mn–Ga foam. Journal of Applied Physics, 2010, 108, .	1.1	24
193	Microstructure development during pack aluminization of nickel and nickel–chromium wires. Intermetallics, 2014, 50, 43-53.	1.8	24
194	Effect of Yb microadditions on creep resistance of a dilute Al-Er-Sc-Zr alloy. Materialia, 2018, 4, 65-69.	1.3	24
195	Creep and Thermal Cycling. , 1993, , 191-214.		23
196	Surface-oxidized, freeze-cast cobalt foams: Microstructure, mechanical properties and electrochemical performance. Acta Materialia, 2018, 142, 213-225.	3.8	23
197	Effect of Si micro-addition on creep resistance of a dilute Al-Sc-Zr-Er alloy. Materials Science & Engineering A: Structural Materials: Properties, Microstructure and Processing, 2018, 734, 27-33.	2.6	23
198	Ni-Al2O3 nacre-like composites through hot-pressing of freeze-cast foams. Materials Science & Engineering A: Structural Materials: Properties, Microstructure and Processing, 2019, 743, 190-196.	2.6	23

#	Article	IF	CITATIONS
199	Effect of micro-additions of Ge, In or Sn on precipitation in dilute Al-Sc-Zr alloys. Materials Science & Engineering A: Structural Materials: Properties, Microstructure and Processing, 2019, 739, 427-436.	2.6	23
200	In situ X-ray synchrotron diffraction study of MgB2 synthesis from elemental powders. Acta Materialia, 2008, 56, 1680-1688.	3.8	22
201	Mechanisms and kinetics of MgB2 synthesis from boron fibers. Acta Materialia, 2008, 56, 5751-5763.	3.8	22
202	Solid-state foaming of Ti–6Al–4V by creep or superplastic expansion of argon-filled pores. Acta Materialia, 2010, 58, 4387-4397.	3.8	22
203	Microstructure and Strength of NiTi-Nb Eutectic Braze Joining NiTi Wires. Metallurgical and Materials Transactions A: Physical Metallurgy and Materials Science, 2015, 46, 1433-1436.	1.1	22
204	Directional solidification of aqueous TiO2 suspensions under reduced gravity. Acta Materialia, 2017, 124, 608-619.	3.8	22
205	Porous Titanium Cylinders Obtained by the Freeze-Casting Technique: Influence of Process Parameters on Porosity and Mechanical Behavior. Metals, 2020, 10, 188.	1.0	22
206	Microstructure and creep properties of cast near-eutectic Al–Ce–Ni alloys. Materials Science & Engineering A: Structural Materials: Properties, Microstructure and Processing, 2022, 833, 142551.	2.6	22
207	Synthesis of superconducting Mg/MgB2 composites. Applied Physics Letters, 2001, 79, 4186-4188.	1.5	21
208	Effect of hafnium micro-addition on precipitate microstructure and creep properties of a Fe-Ni-Al-Cr-Ti ferritic superalloy. Acta Materialia, 2018, 153, 126-135.	3.8	21
209	In operando tomography reveals degradation mechanisms in lamellar iron foams during redox cycling at 800°C. Journal of Power Sources, 2020, 448, 227463.	4.0	21
210	Ultrafine-grained Al-Mg-Zr alloy processed by shear-assisted extrusion with high thermal stability. Scripta Materialia, 2020, 186, 326-330.	2.6	21
211	Effect of Cr additions on a γ-γ' microstructure and creep behavior of a Co-based superalloy with low W content. Materials Science & Engineering A: Structural Materials: Properties, Microstructure and Processing, 2020, 778, 139108.	2.6	21
212	Creep of aluminum syntactic foams. Materials Science & Engineering A: Structural Materials: Properties, Microstructure and Processing, 2008, 488, 573-579.	2.6	20
213	Texture and training of magnetic shape memory foam. Acta Materialia, 2013, 61, 2113-2120.	3.8	20
214	Magnetic-field-induced bending and straining of Ni–Mn–Ga single crystal beams with high aspect ratios. Acta Materialia, 2015, 95, 284-290.	3.8	20
215	Porous shape-memory NiTi-Nb with microchannel arrays. Acta Materialia, 2016, 115, 83-93.	3.8	20
216	Creep behavior and postcreep thermoelectric performance of the n-type half-Heusler alloy Hf0.3Zr0.7NiSn0.98Sb0.02. Materials Today Physics, 2019, 9, 100134.	2.9	20

#	Article	IF	CITATIONS
217	Creating Aligned, Elongated Pores in Titanium Foams by Swaging of Preforms with Ductile Spaceâ€Holder. Advanced Engineering Materials, 2009, 11, 52-55.	1.6	19
218	Atomicâ€Scale Characterization of Aluminumâ€Based Multishell Nanoparticles Created by Solidâ€State Synthesis. Small, 2010, 6, 1728-1731.	5.2	19
219	Enhanced field induced martensitic phase transition and magnetocaloric effect in Ni55Mn20Ga25 metallic foams. Intermetallics, 2011, 19, 952-956.	1.8	19
220	Pack Aluminization Synthesis of Superalloy 3D Woven and 3D Braided Structures. Metallurgical and Materials Transactions A: Physical Metallurgy and Materials Science, 2015, 46, 426-438.	1.1	19
221	Numerical and experimental investigation of (de)lithiation-induced strains in bicontinuous silicon-coated nickel inverse opal anodes. Acta Materialia, 2016, 107, 289-297.	3.8	19
222	Integrated porous cobalt oxide/cobalt anode with micro- and nano-pores for lithium ion battery. Applied Surface Science, 2020, 525, 146592.	3.1	19
223	Diffraction strain measurements in a partially crystallized bulk metallic glass composite containing ductile particles. Journal of Non-Crystalline Solids, 2003, 317, 176-180.	1.5	18
224	Effect of initial preform porosity on solid-state foaming of titanium. Journal of Materials Research, 2006, 21, 1175-1188.	1.2	18
225	Effect of machined feature size relative to the microstructural size on the superelastic performance in polycrystalline NiTi shape memory alloys. Materials Science & Engineering A: Structural Materials: Properties, Microstructure and Processing, 2017, 706, 227-235.	2.6	18
226	Ice-Templated W-Cu Composites with High Anisotropy. Scientific Reports, 2019, 9, 476.	1.6	18
227	Mechanical properties of Ti–W alloys reinforced with TiC particles. Materials Science & Engineering A: Structural Materials: Properties, Microstructure and Processing, 2008, 485, 703-710.	2.6	17
228	Processing and compressive creep of cast replicated IN792 Ni-base superalloy foams. Materials Science & Engineering A: Structural Materials: Properties, Microstructure and Processing, 2012, 558, 129-133.	2.6	17
229	Effects of pore morphology on the cyclical oxidation/reduction of iron foams created via camphene-based freeze casting. Journal of Alloys and Compounds, 2020, 845, 156278.	2.8	17
230	Effects of W and Si microadditions on microstructure and the strength of dilute precipitation-strengthened Al–Zr–Er alloys. Materials Science & Engineering A: Structural Materials: Properties, Microstructure and Processing, 2020, 798, 140159.	2.6	17
231	Metallurgical analysis of copper artifacts from Cahokia. Journal of Archaeological Science, 2011, 38, 1727-1736.	1.2	16
232	Transient liquid-phase bonded 3D woven Ni-based superalloys. Scripta Materialia, 2015, 108, 60-63.	2.6	16
233	Tungsten solubility in L12-ordered Al3Er and Al3Zr nanoprecipitates formed by aging in an aluminum matrix. Journal of Alloys and Compounds, 2020, 820, 153383.	2.8	16
234	Synchrotron X-ray diffraction and imaging of ancient Chinese bronzes. Applied Physics A: Materials Science and Processing, 2006, 83, 163-168.	1.1	15

#	Article	IF	CITATIONS
235	Niobium Wires as Space Holder and Sintering Aid for Porous NiTi. Advanced Engineering Materials, 2011, 13, 301-305.	1.6	15
236	Cast-Replicated NiTiCu Foams with Superelastic Properties. Metallurgical and Materials Transactions A: Physical Metallurgy and Materials Science, 2012, 43, 2939-2944.	1.1	15
237	Modeling of Stresses and Strains during (De)Lithiation of Ni ₃ Sn ₂ -Coated Nickel Inverse-Opal Anodes. ACS Applied Materials & Interfaces, 2017, 9, 15433-15438.	4.0	15
238	Synthesis of precipitation-strengthened Al-Sc, Al-Zr and Al-Sc-Zr alloys via selective laser melting of elemental powder blends. Additive Manufacturing, 2020, 36, 101461.	1.7	15
239	Solute-induced strengthening during creep of an aged-hardened Al-Mn-Zr alloy. Acta Materialia, 2021, 219, 117268.	3.8	15
240	Hydrogen-induced internal-stress plasticity in titanium. Metallurgical and Materials Transactions A: Physical Metallurgy and Materials Science, 2001, 32, 841-847.	1.1	14
241	Kinetics of biaxial dome formation by transformation superplasticity of titanium alloys and composites. Metallurgical and Materials Transactions A: Physical Metallurgy and Materials Science, 2002, 33, 1669-1680.	1.1	14
242	Matisse to Picasso: a compositional study of modern bronze sculptures. Analytical and Bioanalytical Chemistry, 2009, 395, 171-184.	1.9	14
243	Hydrogen-induced transformation superplasticity in zirconium. International Journal of Hydrogen Energy, 2010, 35, 5708-5713.	3.8	14
244	Compressive creep behavior of cast Bi2Te3. Materials Science & Engineering A: Structural Materials: Properties, Microstructure and Processing, 2013, 565, 321-325.	2.6	14
245	Individual and synergistic effects of Mn and Mo micro-additions on precipitation and strengthening of a dilute Al–Zr-Sc-Er-Si alloy. Materials Science & Engineering A: Structural Materials: Properties, Microstructure and Processing, 2021, 800, 140288.	2.6	14
246	Comparing evolution of precipitates and strength upon aging of cast and laser-remelted Al–8Ce-0.2Sc-0.1Zr (wt.%). Materials Science & Engineering A: Structural Materials: Properties, Microstructure and Processing, 2022, 840, 142990.	2.6	14
247	Creep properties and microstructure evolution at 260–300°C of AlSi10Mg manufactured via laser powder-bed fusion. Materials Science & Engineering A: Structural Materials: Properties, Microstructure and Processing, 2022, 843, 143075.	2.6	14
248	A numerical model of transformation superplasticity for iron. Materials Science & Engineering A: Structural Materials: Properties, Microstructure and Processing, 1999, 262, 166-172.	2.6	13
249	In situ synthesis of superconducting MgB2 fibers within a magnesium matrix. Applied Physics Letters, 2003, 83, 120-122.	1.5	13
250	Improving coarsening resistance of dilute Al-Sc-Zr-Si alloys with Sr or Zn additions. Materials Science & Engineering A: Structural Materials: Properties, Microstructure and Processing, 2019, 754, 447-456.	2.6	13
251	Low-density, W-free Co–Nb–V–Al-based superalloys with γ/γ' microstructure. Materials Science & Engineering A: Structural Materials: Properties, Microstructure and Processing, 2020, 796, 139977.	2.6	13
252	High-temperature mechanical properties of γ/γ′ Co–Ni–W–Al superalloy microlattices. Scripta Materialia 2020, 188, 146-150.	'2.6	13

#	Article	IF	CITATIONS
253	Fe–Ni foams self-heal during redox cycling <i>via</i> reversible formation/homogenization of a ductile Ni scaffold. Journal of Materials Chemistry A, 2020, 8, 19375-19386.	5.2	13
254	Microstructure and properties of additively-manufactured WC-Co microlattices and WC-Cu composites. Acta Materialia, 2021, 221, 117420.	3.8	13
255	Internal stress plasticity due to chemical stresses. Acta Materialia, 2001, 49, 3387-3400.	3.8	12
256	Transformation Superplasticity of Cast Titanium and Ti-6Al-4V. Metallurgical and Materials Transactions A: Physical Metallurgy and Materials Science, 2007, 38, 44-53.	1.1	12
257	Porous materials: Less is more. Journal of Materials Research, 2013, 28, 2187-2190.	1.2	12
258	Fabricating Ni–Mn–Ga microtubes by diffusion of Mn and Ga into Ni tubes. Intermetallics, 2014, 49, 70-80.	1.8	12
259	Finite element analysis of mechanical stability of coarsened nanoporous gold. Scripta Materialia, 2016, 115, 96-99.	2.6	12
260	Deposition-based synthesis of nickel-based superalloy microlattices. Scripta Materialia, 2017, 138, 28-31.	2.6	12
261	Multidimensional Anodized Titanium Foam Photoelectrode for Efficient Utilization of Photons in Mesoscopic Solar Cells. Small, 2017, 13, 1701458.	5.2	12
262	Structure and growth of core–shell nanoprecipitates in Al–Er–Sc–Zr–V–Si high-temperature alloys. Journal of Materials Science, 2019, 54, 1857-1871.	1.7	12
263	3D ink-extrusion printing and sintering of Ti, Ti-TiB and Ti-TiC microlattices. Additive Manufacturing, 2020, 35, 101412.	1.7	12
264	Effect of freeze–thaw cycles on load transfer between the biomineral and collagen phases in bovine dentin. Materials Science and Engineering C, 2011, 31, 1423-1428.	3.8	11
265	NiTi porous structure with 3D interconnected microchannels using steel wire spaceholders. Materials Science & Engineering A: Structural Materials: Properties, Microstructure and Processing, 2015, 634, 153-160.	2.6	11
266	The effect of solidification direction with respect to gravity on ice-templated TiO2 microstructures. Journal of the European Ceramic Society, 2019, 39, 3180-3193.	2.8	11
267	Kinetics of alloy formation and densification in Fe-Ni-Mo microfilaments extruded from oxide- or metal-powder inks. Acta Materialia, 2020, 193, 51-60.	3.8	11
268	Microstructure and Hardness of Scandium Trialuminide with Ternary Rare-Earth Additions. Materials Science Forum, 2007, 539-543, 1565-1570.	0.3	10
269	Effect of high-energy X-ray irradiation on creep mechanisms in bone and dentin. Journal of the Mechanical Behavior of Biomedical Materials, 2013, 21, 17-31.	1.5	10
270	Compressive creep behavior of hot-pressed Mg1.96Al0.04Si0.97Bi0.03. Scripta Materialia, 2018, 148, 10-14.	2.6	10

#	Article	IF	CITATIONS
271	Effect of diffusion distance on evolution of Kirkendall pores in titanium-coated nickel wires. Intermetallics, 2019, 104, 124-132.	1.8	10
272	A fully coupled diffusional-mechanical finite element modeling for tin oxide-coated copper anode system in lithium-ion batteries. Computational Materials Science, 2020, 172, 109343.	1.4	10
273	Hierarchical Structural Changes During Redox Cycling of Fe-Based Lamellar Foams Containing YSZ, CeO ₂ , or ZrO ₂ . ACS Applied Materials & Interfaces, 2020, 12, 27190-27201.	4.0	10
274	Increasing γ' volume fraction in Co–Nb–V- and Co–Ta–V-based superalloys. Journal of Materials Research and Technology, 2021, 11, 2305-2313.	2.6	10
275	Internal-stress plasticity in titanium by cyclic alloying/dealloying with hydrogen. Journal of Materials Processing Technology, 2001, 117, 409-417.	3.1	9
276	Superplastic compressive flow in MgB2. Acta Materialia, 2009, 57, 4745-4750.	3.8	9
277	Finite-Element Modeling of Titanium Powder Densification. Metallurgical and Materials Transactions A: Physical Metallurgy and Materials Science, 2012, 43, 381-390.	1.1	9
278	Morphological Study of Directionally Freeze-Cast Nickel Foams. Metallurgical and Materials Transactions E, 2016, 3, 46-54.	0.5	9
279	Dislocation dynamics modeling of precipitation strengthening in Fe–Ni–Al–Cr ferritic superalloys. Journal of Materials Research, 2017, 32, 4241-4253.	1.2	9
280	Dislocation dynamics simulations of precipitation-strengthened Ni- and Co-based superalloys. Materialia, 2018, 1, 211-220.	1.3	9
281	Creep behavior and post-creep thermoelectric performance of the n-type Skutterudite alloy Yb0.3Co4Sb12. Journal of Materiomics, 2021, 7, 89-97.	2.8	9
282	Thermal stability and influence of Y2O3 dispersoids on the heat treatment response of an additively manufactured ODS Ni–Cr–Al–Ti γ/γ′ superalloy. Journal of Materials Research and Technology, 2021, 15 2883-2898.	5,2.6	9
283	Influence of γ′-raft orientation on creep resistance of monocrystalline Co-based superalloys. Materialia, 2020, 12, 100678.	1.3	9
284	Solidification microstructure, aging evolution and creep resistance of laser powder-bed fused Al-7Ce-8Mg (wt%). Additive Manufacturing, 2022, 55, 102862.	1.7	9
285	Microstructure and thermomechanical properties of Al11Ce3. Intermetallics, 2022, 148, 107636.	1.8	9
286	Anisotropic mechanical properties of amorphous Zr-based foams with aligned, elongated pores. Acta Materialia, 2013, 61, 5937-5948.	3.8	8
287	Development of a Precipitation-Strengthened Matrix for Non-quenchable Aluminum Metal Matrix Composites. Jom, 2016, 68, 1915-1924.	0.9	8
288	Effect of aging on coarsening- and creep resistance of a Ti-modified Fe–Ni–Al–Cr–Mo ferritic steel with L21/B2 composite precipitates. Materials Science & Engineering A: Structural Materials: Properties, Microstructure and Processing, 2020, 776, 138987.	2.6	8

#	Article	IF	CITATIONS
289	Interface structure in infiltrated composites of aluminum reinforced with alumina-silica fiber preforms. Metallurgical and Materials Transactions A - Physical Metallurgy and Materials Science, 1991, 22, 1126-1128.	1.4	7
290	Effect of crystalline metallic particles on the compressive behavior of a cellular amorphous metal. Scripta Materialia, 2011, 64, 1031-1034.	2.6	7
291	Amorphous Hf-based foams with aligned, elongated pores. Materials Science & Engineering A: Structural Materials: Properties, Microstructure and Processing, 2012, 533, 124-127.	2.6	7
292	Effect of X-ray irradiation on the elastic strain evolution in the mineral phase of bovine bone under creep and load-free conditions. Acta Biomaterialia, 2013, 9, 5305-5312.	4.1	7
293	Effect of U and Th trace additions on the precipitation strengthening of Al–0.09Sc (at.%) alloy. Journal of Materials Science, 2019, 54, 3485-3495.	1.7	7
294	Evolution of Y2O3 dispersoids during laser powder bed fusion of oxide dispersion strengthened Ni-Cr-Al-Ti γ/γ' superalloy. Additive Manufacturing, 2021, 47, 102224.	1.7	7
295	Methodological aspects of the high-energy synchrotron X-ray diffraction technique for internal stress evaluation. Journal of Neutron Research, 2001, 9, 495-501.	0.4	6
296	Transformation-mismatch plasticity of NiAl/ZrO2 composites — experiments and continuum modeling. Materials Science & Engineering A: Structural Materials: Properties, Microstructure and Processing, 2001, 298, 63-72.	2.6	6
297	Transformation-mismatch plasticity of NiAl/ZrO2 composites—finite-element modeling. Materials Science & Engineering A: Structural Materials: Properties, Microstructure and Processing, 2002, 335, 128-136.	2.6	6
298	Amorphous Zr-Based Foams with Aligned, Elongated Pores. Metallurgical and Materials Transactions A: Physical Metallurgy and Materials Science, 2010, 41, 1706-1713.	1.1	6
299	Effect of stress and temperature on the micromechanics of creep in highly irradiated bone and dentin. Materials Science and Engineering C, 2013, 33, 1467-1475.	3.8	6
300	Development of High-Strength and High-Electrical-Conductivity Aluminum Alloys for Power Transmission Conductors. Minerals, Metals and Materials Series, 2018, , 247-251.	0.3	6
301	Finite Element Model for Coupled Diffusion and Elastoplastic Deformation during High-Temperature Oxidation of Fe to FeO. Journal of the Electrochemical Society, 2020, 167, 080532.	1.3	6
302	Microstructure evolution during reduction and sintering of 3D-extrusion-printed Bi2O3+TeO2 inks to form Bi2Te3. Acta Materialia, 2021, 221, 117422.	3.8	6
303	Tensile Transformationâ€Mismatch Plasticity of Bismuth Sesquioxide. Journal of the American Ceramic Society, 2000, 83, 2521-2528.	1.9	5
304	Transformation Superplasticity in Zircadyne 705. Journal of Materials Engineering and Performance, 2004, 13, 665-669.	1.2	5
305	Copper-zirconium tungstate composites exhibiting low and negative thermal expansion influenced by reinforcement phase transformations. Metallurgical and Materials Transactions A: Physical Metallurgy and Materials Science, 2004, 35, 1159-1165.	1.1	5
306	Superplastic deformation induced by cyclic hydrogen charging. Journal of Applied Physics, 2008, 103, 103518.	1.1	5

#	Article	IF	CITATIONS
307	Transformation mismatch plasticity in Pd induced by cyclic hydrogen charging. Materials Science & Engineering A: Structural Materials: Properties, Microstructure and Processing, 2009, 523, 178-183.	2.6	5
308	Concurrent Growth of Kirkendall Pores and Vapor–Solid–Solid Protuberances on Ni Wires During Mo Vapor-Phase Deposition. Metallurgical and Materials Transactions A: Physical Metallurgy and Materials Science, 2014, 45, 6252-6259.	1.1	5
309	Effect of cyclic loading on the nanoscale deformation of hydroxyapatite and collagen fibrils in bovine bone. Biomechanics and Modeling in Mechanobiology, 2014, 13, 615-626.	1.4	5
310	Microstructure Evolution During Al, Ti, and Mo Surface Deposition and Volume Diffusion in Ni-20Cr Wires and Woven Structures. Metallurgical and Materials Transactions A: Physical Metallurgy and Materials Science, 2015, 46, 2249-2254.	1.1	5
311	In operando X-ray diffraction strain measurement in Ni3Sn2 – Coated inverse opal nanoscaffold anodes for Li-ion batteries. Journal of Power Sources, 2017, 367, 80-89.	4.0	5
312	Effects of W micro-additions on precipitation kinetics and mechanical properties of an Al–Mn–Mo–Si–Zr–Sc–Er alloy. Materials Science & Engineering A: Structural Materials: Properties, Microstructure and Processing, 2021, 803, 140550.	2.6	5
313	Complex-shaped, finely-featured ZrC/W composites via shape-preserving reactive melt infiltration of porous WC structures fabricated by 3D ink extrusion. Additive Manufacturing Letters, 2021, 1, 100018.	0.9	5
314	Evolution of lamellar architecture and microstructure during redox cycling of Fe-Co and Fe-Cu foams. Journal of Alloys and Compounds, 2022, 918, 165606.	2.8	5
315	Effect of Y2O3 dispersoids on microstructure and creep properties of Hastelloy X processed by laser powder-bed fusion. Additive Manufacturing Letters, 2022, 3, 100069.	0.9	5
316	Effects of Ni and Cr additions on γ + γ' microstructure and mechanical properties of W-free Co–Al–V–Nb–Ta-based superalloys. Materials Science & Engineering A: Structural Materials: Properties, Microstructure and Processing, 2022, 849, 143401.	2.6	5
317	Microstructural evolution of lamellar Fe-25Ni foams during steam-hydrogen redox cycling. Acta Materialia, 2022, 237, 118148.	3.8	5
318	Transformation-mismatch plasticity in sub-millimeter iron wires. Materials Science & Engineering A: Structural Materials: Properties, Microstructure and Processing, 2006, 421, 35-39.	2.6	4
319	Recent Developments in Ni-Mn-Ga Foam Research. Materials Science Forum, 0, 635, 119-124.	0.3	4
320	Metallic sandwiches with open porosity facings and closed porosity cores for SOFC interconnects. Materials Science & Engineering A: Structural Materials: Properties, Microstructure and Processing, 2013, 585, 32-38.	2.6	4
321	3D-printed tungsten sheet-gyroids via reduction and sintering of extruded WO3-nanopowder inks. Additive Manufacturing, 2020, 36, 101613.	1.7	4
322	SnO2-Ag composites with high thermal cycling stability created by Ag infiltration of 3D ink-extruded SnO2 microlattices. Applied Materials Today, 2020, 21, 100794.	2.3	4
323	Introduction - Porous Metals: From Nano to Macro. Journal of Materials Research, 2020, 35, 2529-2534.	1.2	4
324	Microstructural stability and mechanical behavior of a Co–20Ni–7Al–7W–4Ti at.% superalloy. Journal of Alloys and Compounds, 2020, 848, 156378.	2.8	4

#	Article	IF	CITATIONS
325	Microstructure and mechanical properties of 3D ink-extruded CoCrCuFeNi microlattices. Acta Materialia, 2022, 238, 118187.	3.8	4
326	Enhanced densification of cavitated dispersion-strengthened aluminum by thermal cycling. Metallurgical and Materials Transactions A: Physical Metallurgy and Materials Science, 2000, 31, 2647-2657.	1.1	3
327	Synchrotron X-Ray Study of Texture in Cold-Worked Shape-Memory NiTi-Wires. Materials Research Society Symposia Proceedings, 2001, 678, 261.	0.1	3
328	Effect of processing variables on the reaction kinetics of MgB2 fibers. Physica C: Superconductivity and Its Applications, 2010, 470, 648-653.	0.6	3
329	Diffusion Bonding of Ti-6Al-4V Sheet with Ti-6Al-4V Foam for Biomedical Implant Applications. Metallurgical and Materials Transactions B: Process Metallurgy and Materials Processing Science, 2013, 44, 1554-1559.	1.0	3
330	Evolution of Phase Strains During Tensile Loading of Bovine Cortical Bone. Advanced Engineering Materials, 2013, 15, 238-249.	1.6	3
331	Metallic Printing: Metallic Architectures from 3D-Printed Powder-Based Liquid Inks (Adv. Funct.) Tj ETQq1 1 0.784	4314 rgBT 7.8	/Qverlock 10
332	Ice-templated silicon foams with aligned lamellar channels. MRS Communications, 2017, 7, 928-932.	0.8	3
333	Processing and Characterization of Liquid-Phase Sintered NiTi Woven Structures. Shape Memory and Superelasticity, 2018, 4, 70-76.	1.1	3
334	Scandium-Enriched Nanoprecipitates in Aluminum Providing Enhanced Coarsening and Creep Resistance. Minerals, Metals and Materials Series, 2018, , 1589-1594.	0.3	3
335	Experimental and modeling study of compressive creep in 3D-woven Ni-based superalloys. Acta Materialia, 2018, 155, 236-244.	3.8	3
336	Microstructure and compressive properties of 3D-extrusion-printed, aluminized cobalt-based superalloy microlattices. Materials Science & Engineering A: Structural Materials: Properties, Microstructure and Processing, 2021, 815, 141262.	2.6	3
337	Kirkendall pore evolution during interdiffusion and homogenization of titanium-coated nickel microwires. Intermetallics, 2021, 134, 107199.	1.8	3
338	Mechanical properties of meteoritic Fe–Ni alloys for in-situ extraterrestrial structures. Acta Astronautica, 2021, 189, 465-475.	1.7	3
339	Finite element modeling of creep deformation in dendritic alloys. Materials Science & Engineering A: Structural Materials: Properties, Microstructure and Processing, 2022, 831, 142171.	2.6	3
340	Operando X-ray diffraction study of thermal and phase evolution during laser powder bed fusion of Al-Sc-Zr elemental powder blends. Additive Manufacturing, 2022, 55, 102806.	1.7	3
341	The Effect of Dopant Additions on the Microstructure of Boron Fibers Before and After Reaction to MgB2. Materials Research Society Symposia Proceedings, 2004, 848, 326.	0.1	2
342	Blended elemental powder densification of Ti-6Al-4V by hot pressing. Journal of Materials Research, 2011, 26, 965-969.	1.2	2

#	Article	IF	CITATIONS
343	Acoustic Emission Analysis of Damage during Compressive Deformation of Amorphous Zr-Based Foams with Aligned, Elongated Pores. Metallurgical and Materials Transactions A: Physical Metallurgy and Materials Science, 2013, 44, 3114-3122.	1.1	2
344	Enhanced densification of Ti-6Al-4V/TiC powder blends by transformation mismatch plasticity. Journal of Materials Research, 2013, 28, 2520-2527.	1.2	2
345	Nanoscale Cellular Structures at Phase Boundaries of Ni-Cr-Al-Ti and Ni-Cr-Mo-Al-Ti Superalloys. Metallurgical and Materials Transactions A: Physical Metallurgy and Materials Science, 2015, 46, 2680-2687.	1.1	2
346	A Simple and Economical Device to Process Ti Cylinders with Elongated Porosity by Freeze-Casting Techniques: Design and Manufacturing. Key Engineering Materials, 0, 770, 255-261.	0.4	2
347	Evolution of directionally freeze-cast Fe2O3 and Fe2O3+NiO green bodies during reduction and sintering to create lamellar Fe and Fe-20Ni foams. Journal of Alloys and Compounds, 2021, 889, 161707.	2.8	2
348	Effect of oxide dispersoids on precipitation-strengthened Al-1.7Zr (wt %) alloys produced by laser powder-bed fusion. Additive Manufacturing, 2022, 56, 102933.	1.7	2
349	Internal Stresses in Bulk Metallic Glass Matrix Composites. Materials Research Society Symposia Proceedings, 2000, 644, 931.	0.1	1
350	Tensile creep properties of δ-Bi2O3. Scripta Materialia, 2000, 43, 1033-1038.	2.6	1
351	Hydrogen-induced internal-stress plasticity in titanium. Metallurgical and Materials Transactions A: Physical Metallurgy and Materials Science, 2001, 32, 841-843.	1.1	1
352	Oxidation and Creep Behavior of Porous E-Brite for Solid-Oxide Fuel Cell Interconnects. ECS Transactions, 2009, 25, 1361-1368.	0.3	1
353	Light-Weight, Fast-Cycling, Shape-Memory Actuation Structures. , 2011, , .		1
354	Microstructure and Mechanical Properties of an Al-Zr-Er High Temperature Alloy Microalloyed with Tungsten. Minerals, Metals and Materials Series, 2019, , 379-383.	0.3	1
355	Bi2Te3 filaments via extrusion and pressureless sintering of Bi2Te3-based inks. MRS Communications, 2021, 11, 818-824.	0.8	1
356	Longitudinal Relaxation of a Thermally Stressed Fiber by Prismatic Dislocation Punching. Materials Research Society Symposia Proceedings, 1990, 209, 305.	0.1	0
357	Synchrotron X-ray Diffraction Measurement of Reinforcement Strains in Uniaxially Stressed Bulk Metallic Glass Composites. Materials Research Society Symposia Proceedings, 2001, 678, 231.	0.1	0
358	Internal Strain Measurements and X-ray Imaging in Interpenetrating-Phase Al2O3/Al Composites. Materials Research Society Symposia Proceedings, 2004, 840, Q7.10.1.	0.1	0
359	High Energy X-ray Diffraction Measurement of Load Transfer between Hydroxyapatite and Collagen in Bovine Dentin. Materials Research Society Symposia Proceedings, 2009, 1187, 140.	0.1	0
360	Effect of Oxidation on Creep Strength and Resistivity of Porous Fe-26Cr-1Mo. Metallurgical and Materials Transactions E, 2014, 1, 303-310.	0.5	0

#	Article	IF	CITATIONS
361	Equal Channel Angular Pressing of a Newly Developed Precipitation Hardenable Scandium Containing Aluminum Alloy. Minerals, Metals and Materials Series, 2018, , 423-429.	0.3	Ο
362	Mechanical Behavior of Three-Dimensional Braided Nickel-Based Superalloys Synthesized via Pack Cementation. Metallurgical and Materials Transactions A: Physical Metallurgy and Materials Science, 2018, 49, 817-821.	1.1	0
363	Effects of Zr Additions on Structure and Microhardness Evolution of Eutectic Al-6Ni Alloy. Minerals, Metals and Materials Series, 2019, , 373-377.	0.3	0
364	Microstructure and Mechanical Properties of a Precipitation-Hardened Al–Mn–Zr–Er Alloy. Minerals, Metals and Materials Series, 2021, , 239-244.	0.3	0
365	Bulk Nanostructured Metal from Multiply-Twinned Nanowires. Nano Letters, 2021, 21, 5627-5632.	4.5	0
366	Microstructure and Creep Performance of a Multicomponent Co-Based L1 ₂ -Ordered Intermetallic Alloy. SSRN Electronic Journal, 0, , .	0.4	0